

https://dspace.org/

Development of carbon nanotube/platinum electrocatalytic electrodes for proton exchange membrane fuel cell

Afolabi, Ayo Samuel

2010-03-10T07:10:24Z
http://hdl.handle.net/10539/7652

Downloaded from a DSpace repository. https://dspace.org/

4.0 OPTIMIZATION STUDIES FOR CARBON NANOTUBE PRODUCTION

For simplicity, the results and discussion of this research have been divided into two major parts. This chapter reports the first part of these results and discussion, and focused on the analyses of the experimental results obtained on the synthesis of carbon nanotubes using both the SFCCVD and horizontal CVD reactors. It also discusses the analyses of the characterization of these nanomaterials, and a brief description of the equipment used for the characterization and purification for both SFCCVD and horizontal CVD reactors used for the production of these materials. The optimization of the production parameters in the swirled floating catalyst chemical vapour deposition reactor is also discussed in this chapter.

4.1 Synthesis of Carbon Nanotubes by SFCCVD

A series of experiments were carried out to synthesize CNTs at different operating conditions by SFCCVD. This study was undertaken to evaluate the effects of various parameters on the production rate of CNTs and to optimize these parameters. The reaction of acetylene and ferrocene catalyst yielded a complex mixture of carbon particles containing amorphous carbon and carbon nanotubes. Figure 4.1 (a) shows a typical TEM image of good quality, elongated and clean as–synthesized CNTs obtained at 1000°C using an acetylene to hydrogen flow ratio of one to five while Figure 4.1 (b) shows the SEM image of an analogous clustered CNT sample. These CNT samples have an average inner diameter of between 20 and 70 nm while their average length is as long as 10 mm (Abdulkareem *et al.*, 2007; Iyuke *et al*., 2007).

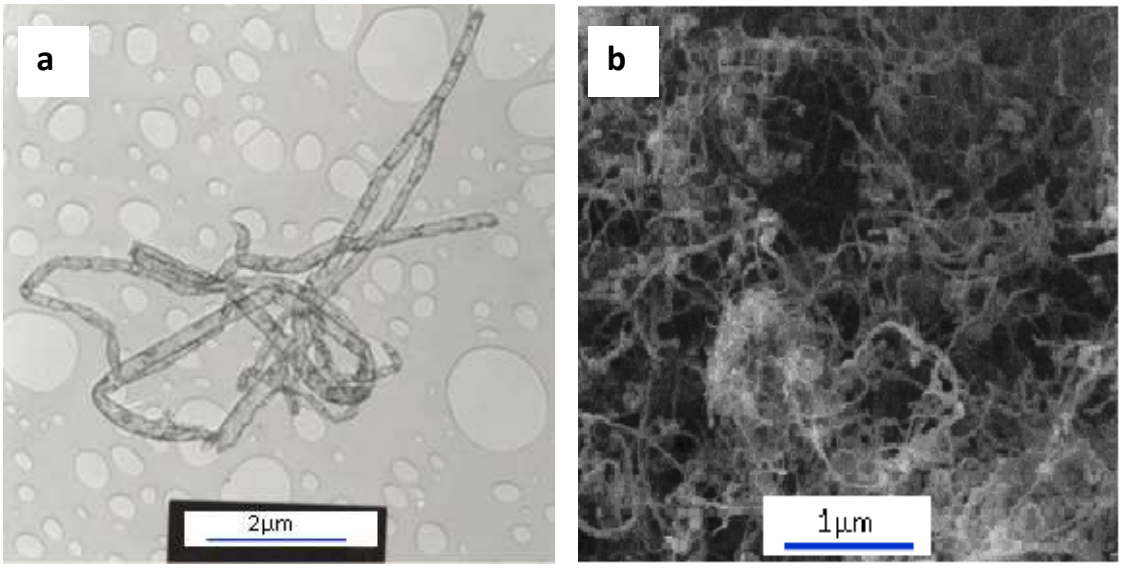

Figure 4.1 (a) TEM image of a long and pure CNT sample obtained at 1000°C. (b) SEM image of clustered CNT samples.

The mechanism of formation of the CNTs is assumed to be similar to that explained by Chen *et al.* (2006), Das *et al.* (2006), Fan *et al.* (2006) and Huang *et al.* (2007) in which the iron catalyst was responsible for the nucleation and growth of the CNTs at the acetylene decomposition temperature. The particle size of the catalyst determines to a large extent the diameter of the nanotubes formed. Ferrocene acted as a precursor for iron which is the catalyst that formed the nucleation sites for the formation of the tubes which subsequently grew at high temperature. Some of these iron particles remained unreactive at low residence time and constituted impurities in the synthesized CNTs. A low decomposition temperature also resulted into the formation of amorphous impurities within these materials.

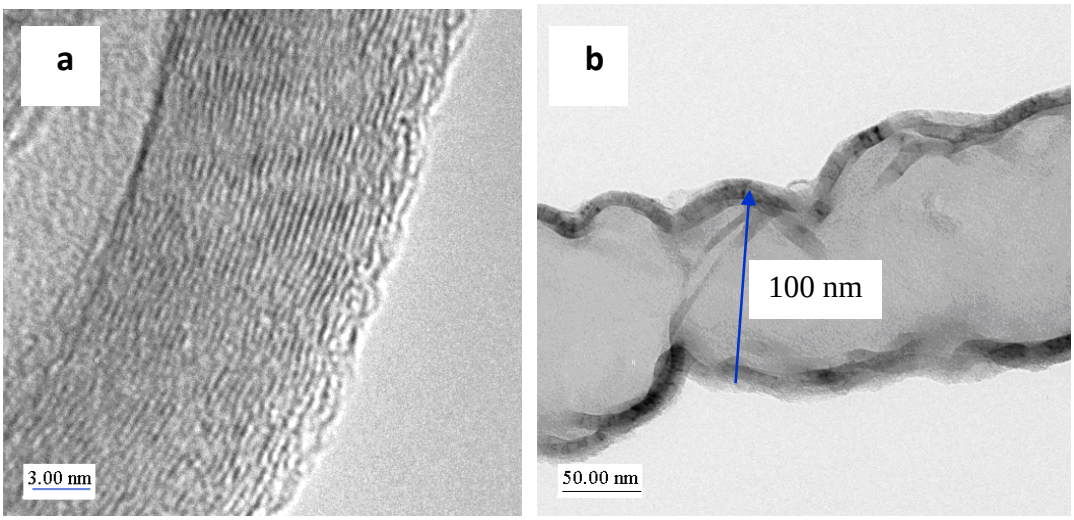

Figure 4.2: (a) TEM image of a CNT sample showing the multi walls (b) High magnification TEM image of CNT sample showing the diameter of the tube.

Figure 4.2 (a) shows a TEM image of a CNT sample showing the thickness of the walls. It can be seen that this sample has multi walls and the average distance between these walls is about 0.34 nm. The high magnification TEM image of the CNT sample shown in Figure 4.2 (b) indicates the diameter of the tube which is about 100 nm.

The XRD pattern of the as-synthesized CNT sample is shown in Figure 4.3. This pattern reveals the characteristic pattern of graphitised carbon which is similar to the ones reported by Zhang *et al*, (2005a) and Kong and Zhang, (2007). The (002) graphitic line observed at 25.8^{o} corresponding to an inter-planner spacing of about 0.343 nm which is usually attributed to graphite. This pattern also indicates a high degree of crystallinity which suggests a low content of amorphous carbon and impurities from the catalyst

which are usually iron particles (Wu *et al*., 2007). While other minor peaks are noise arising from these impurities.

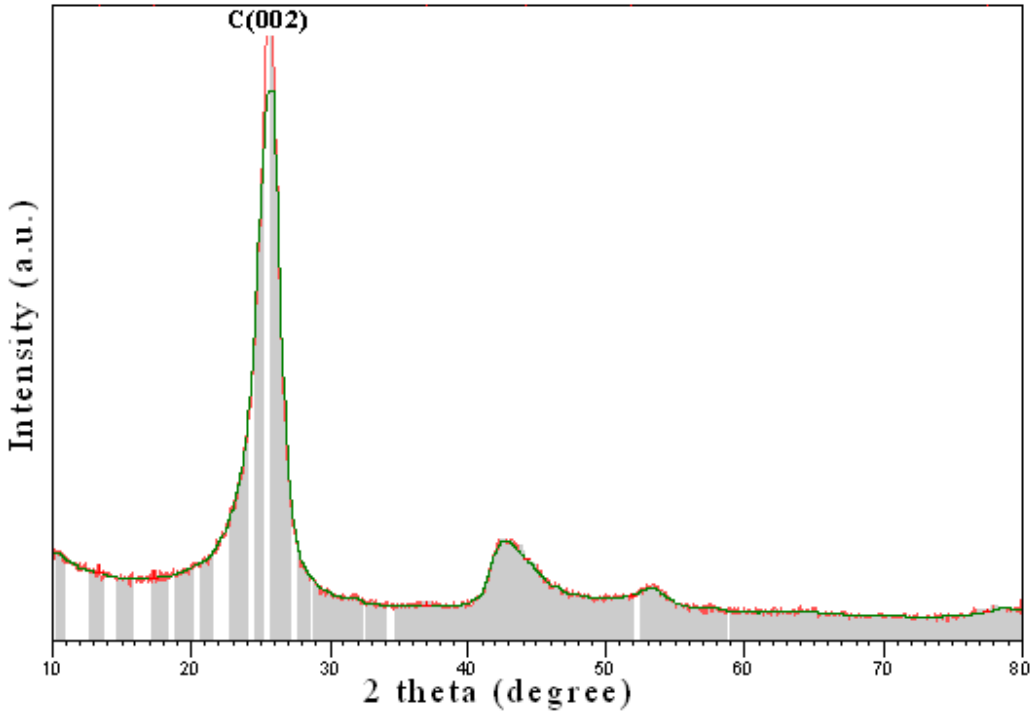

Figure 4.3: XRD pattern of raw CNT sample.

4.1.2 Optimization of SFCCVD production parameters

In order to study and optimize the effects of the operating parameters on the CNT production rate using the SFCCVD equipment, the decomposition temperature, hydrogen flow, acetylene flow and argon flow rates were varied. The temperature (900, 950, 1000 and 1050°C), hydrogen flow rate (118, 181 and 248 ml/min) and acetylene flow rate (181, 248, 308 and 370 ml/min) were varied.

4.1.2.1 Effect of acetylene flow rate

The rate of production of CNTs as a function of acetylene flow rate at various decomposition temperatures and constant flow rate of hydrogen at 118 ml/min is presented in Figure 4.4. It is observed from the Figure that the rate of production of CNTs increases with increase in acetylene flow rate within the range of 188 – 248 ml/min at all temperatures except at 950°C where the production rate decreases within this flow rate range and increased again. The result also shows that as flow rate of acetylene increases from 308 – 370 ml/min, the production rate of CNTs decreases at a reaction temperature of 1000°C.

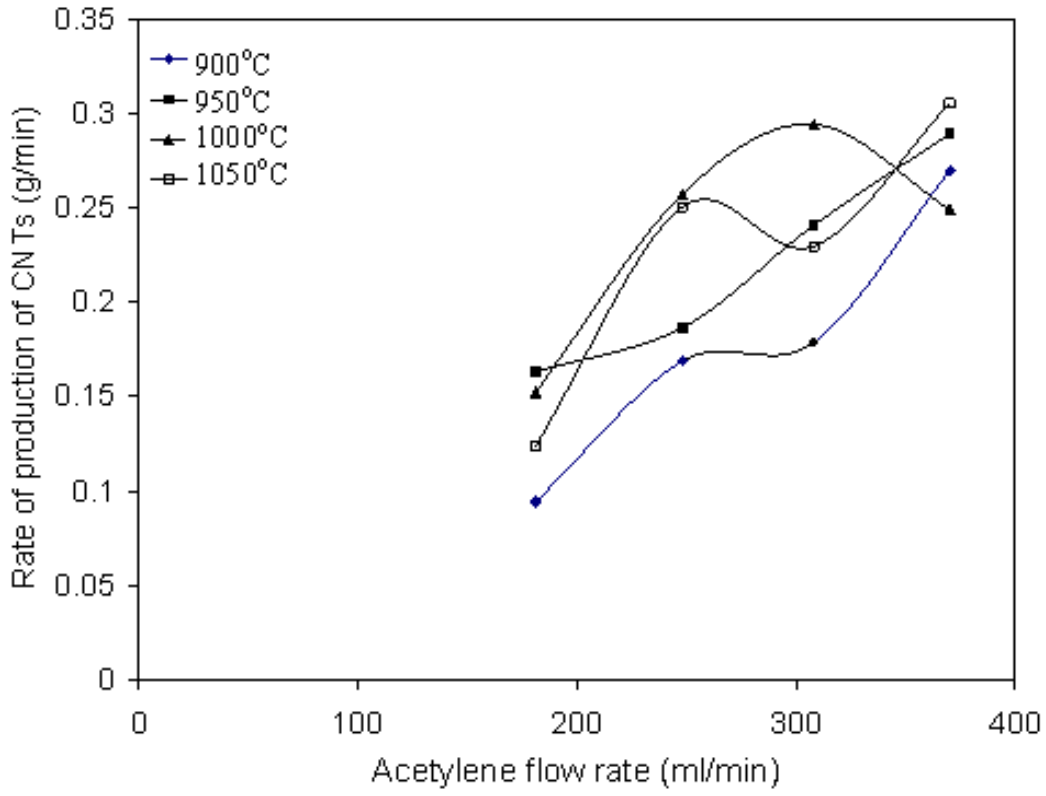

Figure 4.4: Effect of acetylene flow rate on the rate of production of CNTs.

4.1.2.2 Effect of hydrogen flow rate

The effect of hydrogen flow rate on the production of CNTs at constant acetylene flow rate and various reaction temperatures is shown in Figure 4.5. Hydrogen has the ability to either suppress or accelerate the formation of CNTs by creating a velocity profile in the reactor. Hydrogen also affects the formation of the catalyst and the growth of CNTs (Singh *et al.,* 2003). It is observed from the figure that as the hydrogen flow rate increases from 118 to 181 ml/min, the rate of production of CNTs increases at temperatures of 950°C and 1050°C and beyond a flow rate of 181 ml/min, the production rate decreases, while the production rate of CNTs decreases as the flow rate of hydrogen increases at reaction temperatures of 900°C and 1000°C. The findings of Singh *et al.,* (2003) suggest that the reduction in rate of production of CNTs at higher hydrogen flow rate could be attributed to a low residence time of acetylene in the reactor as a result of a high velocity profile created by high hydrogen flow rate, suppresses the formation of CNTs by removing acetylene at a faster rate from the reaction zone of the reactor.

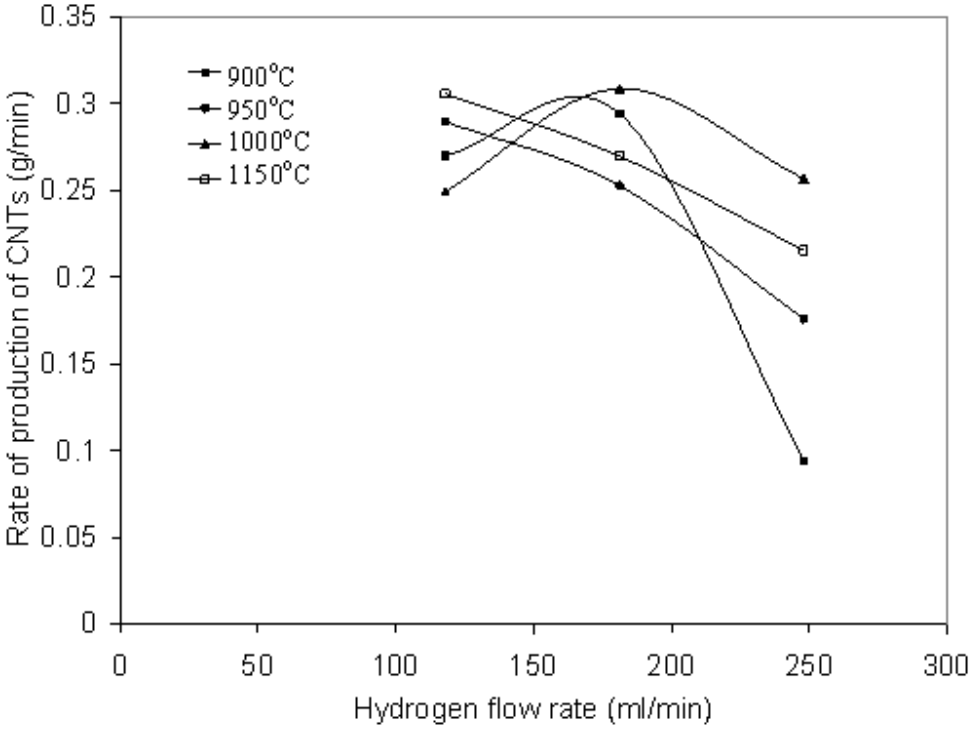

Figure 4.5: Effect of hydrogen flow rate on the rate of production of CNTs.

4.1.2.3 Effect of acetylene to hydrogen flow ratio

The effect of the acetylene/hydrogen flow ratio on the rate of production of CNTs at various temperatures was investigated and the results obtained are shown in Figure 4.6 (Abdulkareem *et al.*, 2007). It can be observed from the Figure that the results are similar at all temperatures except at 950°C where there is only one maximum, but in all cases the rate of production of CNTs increases as the ratio of acetylene/hydrogen ratio increases. The minimum production rate of CNTs was observed at flow ratio of 1 except at 900°C where the minimum production rate was obtained at a flow ratio of 6 (Abdulkareem *et*

al., 2007). However, the effect of flow of acetylene on the size and morphology of CNTs was not investigated in this study.

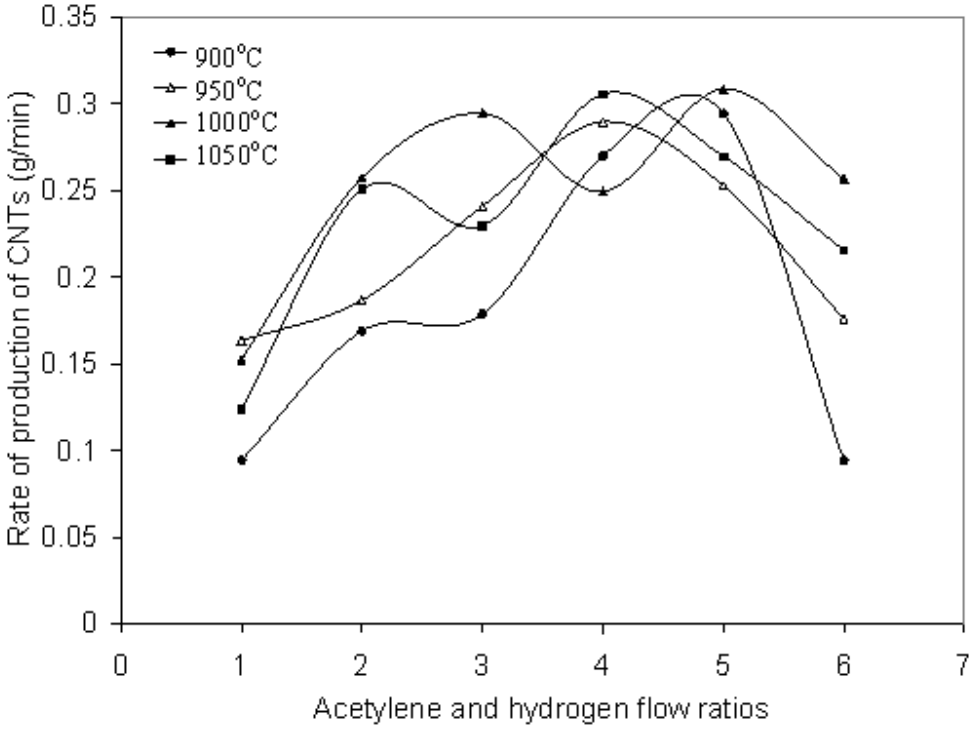

Figure 4.6: Effect of acetylene/hydrogen flow ratio on the rate of production of CNTs.

CNT samples of good quality were collected, similar to that shown in Figure 4.1 (a), at an acetylene to hydrogen flow ratio of 5 (CNT production rate of 0.31 g/min). The patterns of these results explain the influence of hydrogen in the production of CNTs. Apart from creating a velocity profile in the reactor, hydrogen also assisted in reducing ferrocene to atomic iron clusters or nanoparticles. According to Ci *et al.* (2001), the suppressing effect of hydrogen on the synthesis of CNTs is thermodynamic in nature. Hence, hydrogen produces the reverse reaction for decomposition because the gasification of the deposited carbon by hydrogen forms methane (equation 4.1) (Iyuke, 2007). A mechanism based on

3 parallel reactions is proposed for the synthesis of CNTs from acetylene. At high temperatures, acetylene dissociates to carbon and hydrogen vapour and the former are adsorbed onto the surface of the catalyst thereby leading to the formation of C-C bonds and graphene layers.

$$\left.\begin{array}{l} C_2H_2 \rightarrow 2C + H_2 \\ C_2H_2 + 3H_2 \rightarrow 2CH_4 \\ 2CH_4 \rightarrow 2C + 4H_2 \\ \textit{The overall reaction is} \\ 2C_2H_2 \rightarrow 4C + 2H_2 \end{array}\right] nC \xrightarrow{Fe,H_2} C_n - Fe \xrightarrow{c-c_{bond}} CNTs + Fe + H_2 \qquad (4.1)$$

4.1.2.4 Effect of temperature

The results obtained on the effect of temperatures on the rate of production of CNTs at different flow ratios of acetylene and hydrogen is shown in Figure 4.7. The decomposition temperatures were varied between 900 – 1050°C for different flow ratios. It can be observed from the figure that the rate of production of CNTs at different flow ratios of acetylene and hydrogen is influenced significantly by the temperature. As the temperature increases, the quantity of CNTs produced also increases. This indicates that at higher temperature, there is enough heat to effect the decomposition of acetylene leading to the formation of CNTs (Abdulkareem *et al.*, 2007). It was observed during the collection of samples that as the temperature of CNTs increased the quantity of glassy carbon produced also increased in the reactor, while at 900°C and low flow rate of acetylene and hydrogen some shiny tiny diamond-like particles were produced but they are thermodynamically unstable and disappeared after a few minutes.

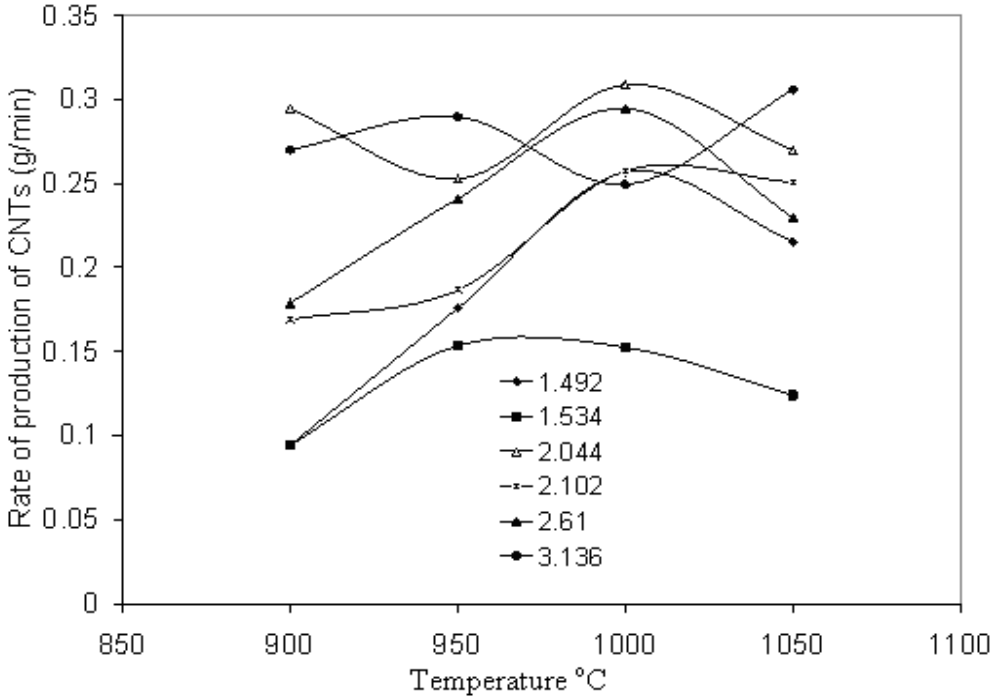

Figure 4.7: Effect of temperature on the rate of production of CNTs at different acetylene/hydrogen flow ratios.

The effects of operational conditions such as temperature, flow rates of acetylene and hydrogen on the production rate of nanoparticles were investigated between the range of 500-1150°C, 180-415 ml/min and 181-343 ml/min respectively, while the flow rate of Ar used as the carrier was 343 ml/min. Figure 4.8 presents the effects of these operating conditions on the amount of CNTs produced at an average period of 615.5 seconds and ferrocene vaporised constantly from an initially feed amount of 5 g.

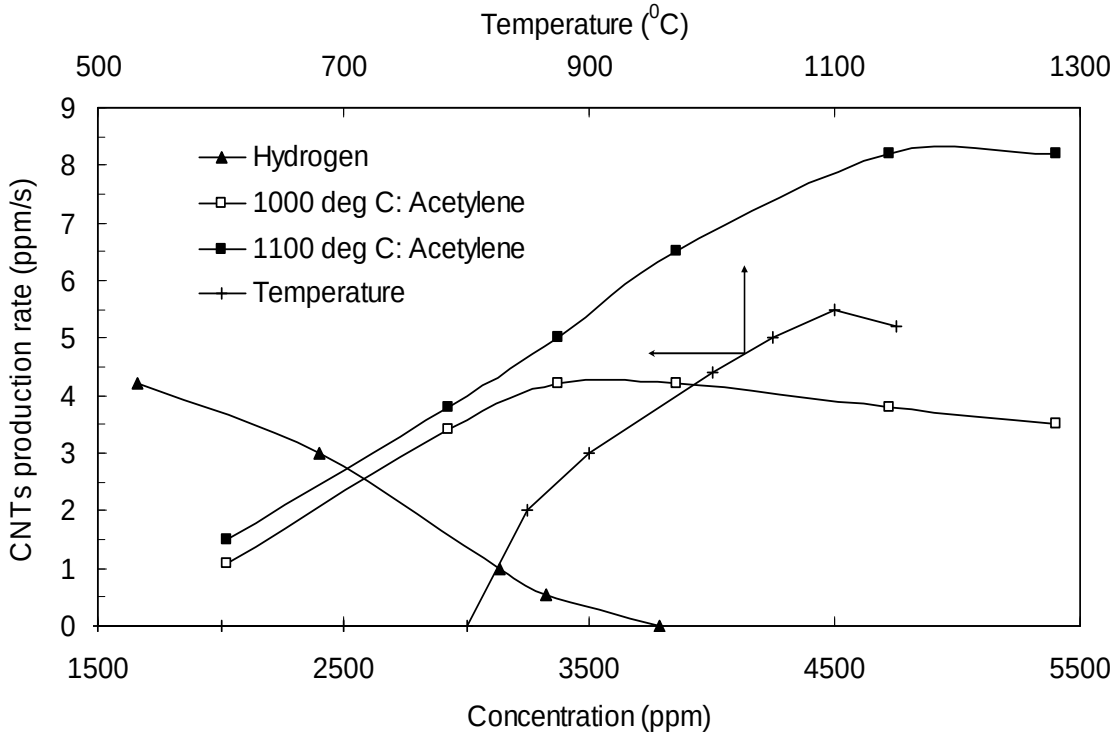

Figure 4.8: Effects of operating conditions on amount of CNTs produced.

It can be seen that CNT production was not observed at temperatures from 500-800°C. Production only started from 850°C at 2 ppm/s with increasing production rate till 1100°C at 5.5 ppm/s, but dropped at 1150°C to 5.2 ppm/s. The decrease in production rate at 1150°C may be due to the thermodynamic stability of the CNTs in the continuous presence of fresh Fe catalyst. This implies that CNT production was favoured from 850-1100°C.

The effect of varying acetylene concentrations at two different operating temperatures of 1000 and 1100°C was also investigated and the results obtained are presented in Figure

4.8. These results revealed similar production trends from 2025 ppm of C_2H_2 to 3375 ppm. The maximum production rate was observed after 3375 ppm of acetylene at 1000°C, while similar pattern was seen at 4725 ppm acetylene at 1100°C. An optimum production rate of 8.2 ppm/s was attained at 1100°C and acetylene feed of 4725 ppm. The effect of hydrogen flow rate on the rate of production of CNTs is also shown in Figure 4.8. It can be seen from Figure 4.8 that an increase in hydrogen from 1661 – 3786 ppm decreased the production rate monotonically from 4.2 ppm/s to zero. At concentration less than 1661 ppm, lumps of amorphous carbons were seen under TEM observation (not shown). These observations are in cognisance with an earlier claim by Singh and co-workers (2003) on the effect of hydrogen concentration on CNT production using the CVD technique. Hence the entire experiments were run at 181 ml/min giving a corresponding hydrogen concentration of 1662 ppm.

4.3 Synthesis of CNTs in a Horizontal CVD Reactor

Unlike in the case of SFCCVD, the horizontal CVD uses nitrogen gas as carrier gas and a bimetallic catalyst. The catalyst which was prepared in the laboratory contains Fe and Co supported on $CaCO_3$ support. The optimisation and the effect of the various production parameters and detailed description of mechanism of formation of CNTs in this equipment have been described (Mhlanga, 2009). Figure 4.9 shows the mass of the catalyst used and the corresponding quantity of the CNTs synthesized under the same reaction conditions: temperature (700°C); flow rate of acetylene (90 ml/min) and nitrogen (240 ml/min); and reaction time (60 minutes). The result indicates that the larger the

amount of catalyst used the higher the CNT yield. The mass of the catalyst was restricted by the size of quartz boat (120 mm X 15 mm) used to synthesise these materials.

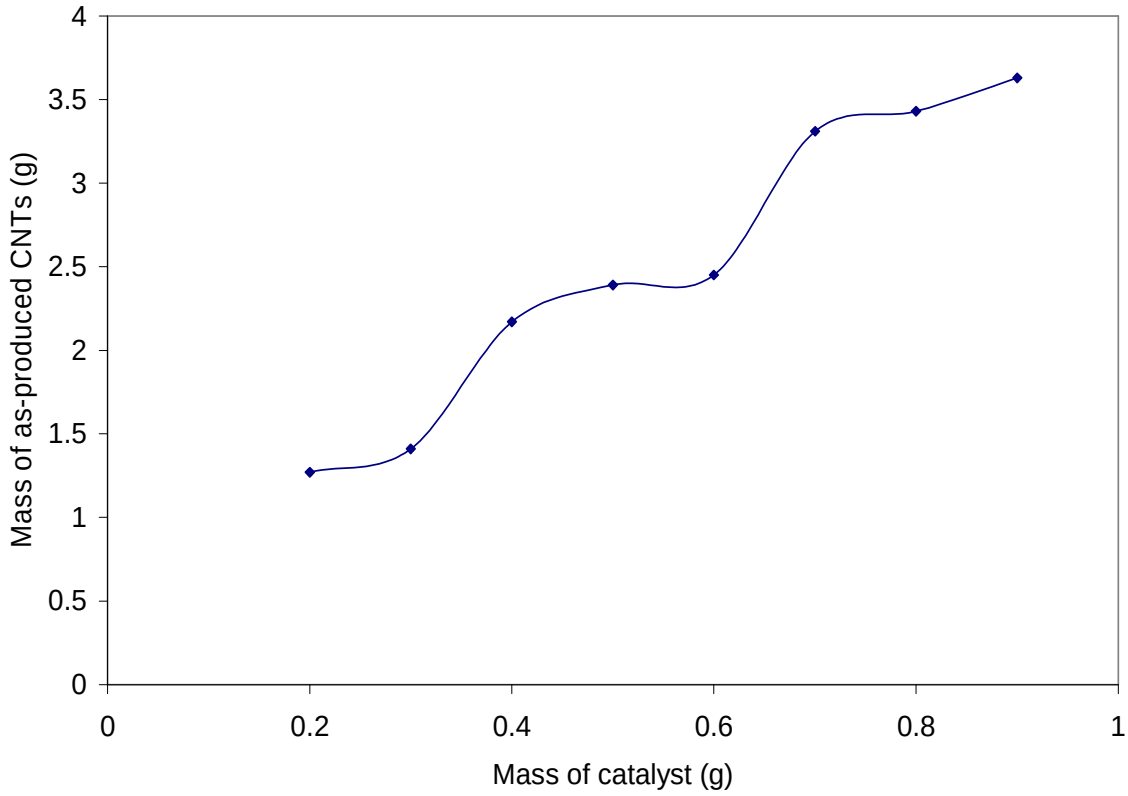

Figure 4.9: Effect of mass of catalyst on the quantity of as-produced CNTs.

Figure 4.10 shows the TEM images of CNT samples produced in this study. These samples are relatively free of amorphous impurities but contain traces of iron and cobalt particles which are clearly detected by EDX analysis (Figure 4.11). These metal impurities are the residue catalyst metals trapped in the matrix of these tubes during

production. Figure 4.12 shows a CNT sample which has inner and outer diameters of 9.2 and 17.9 nm respectively.

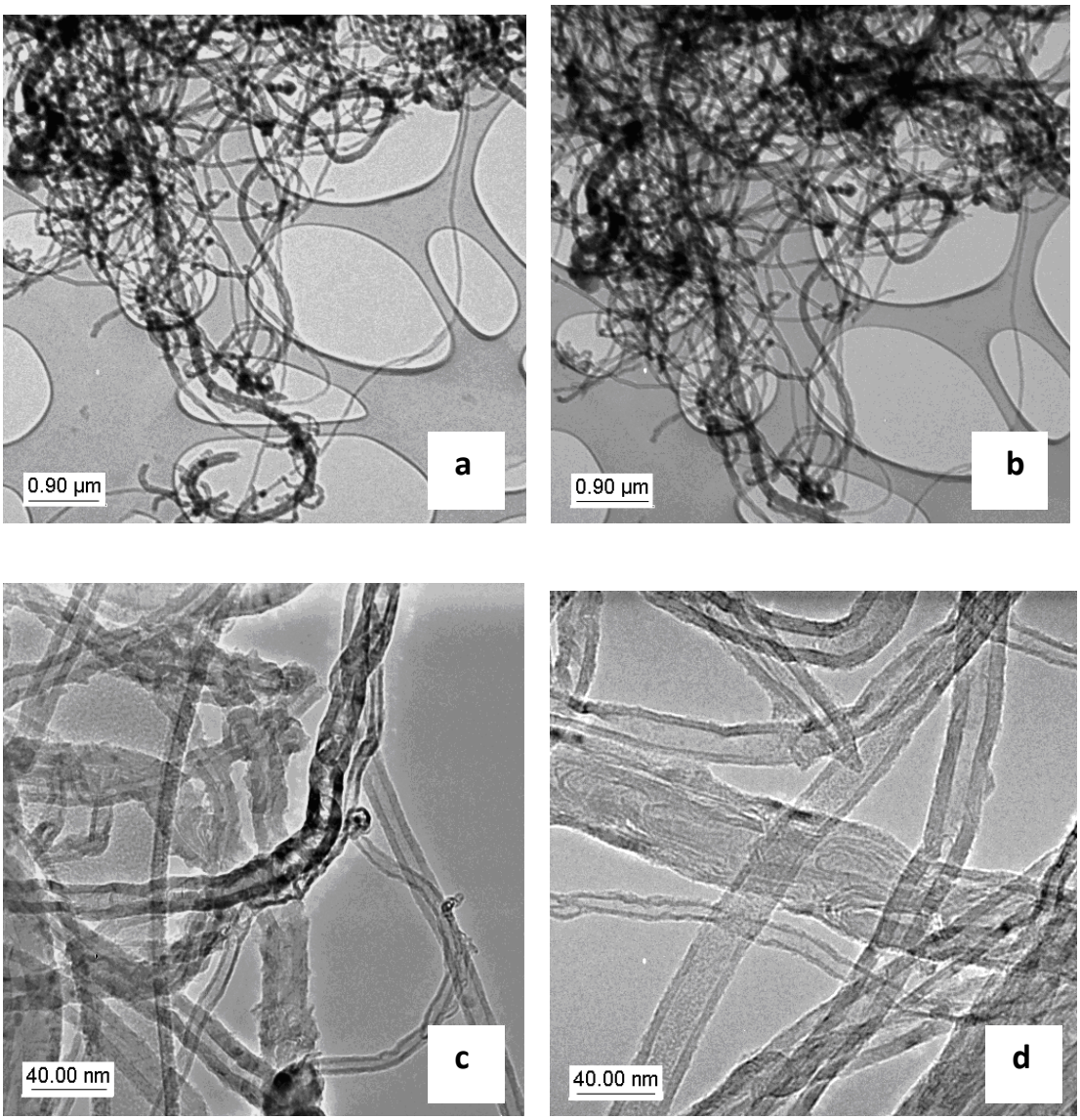

Figure 4.10: (a-b) TEM images of as-produced clustered CNT samples synthesized by horizontal CVD reactor. (c-d) High magnification TEM images of raw CNT samples synthesized by horizontal CVD reactor.

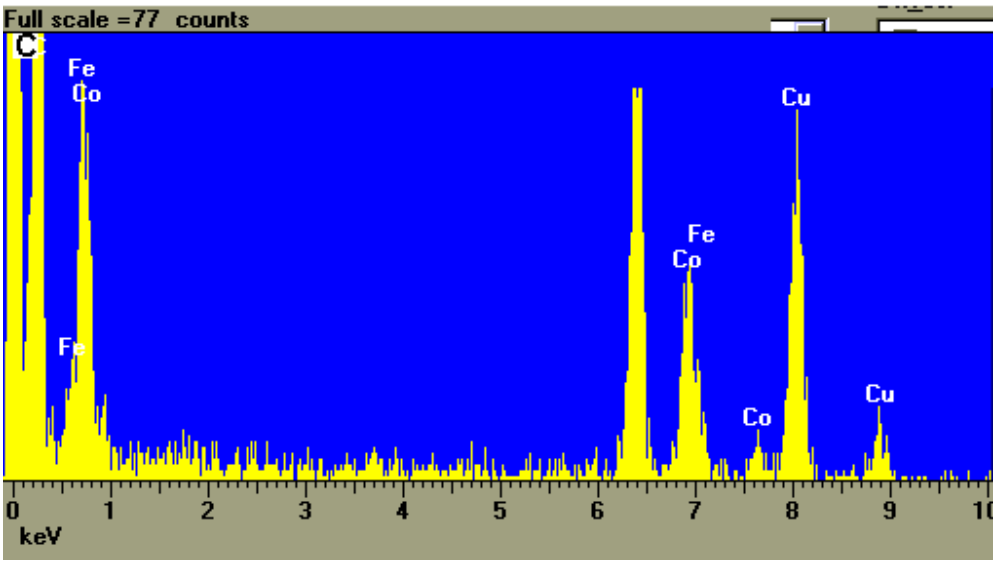

Figure 4.11: EDX analysis of as-synthesized CNT sample showing the presence of Fe and Co

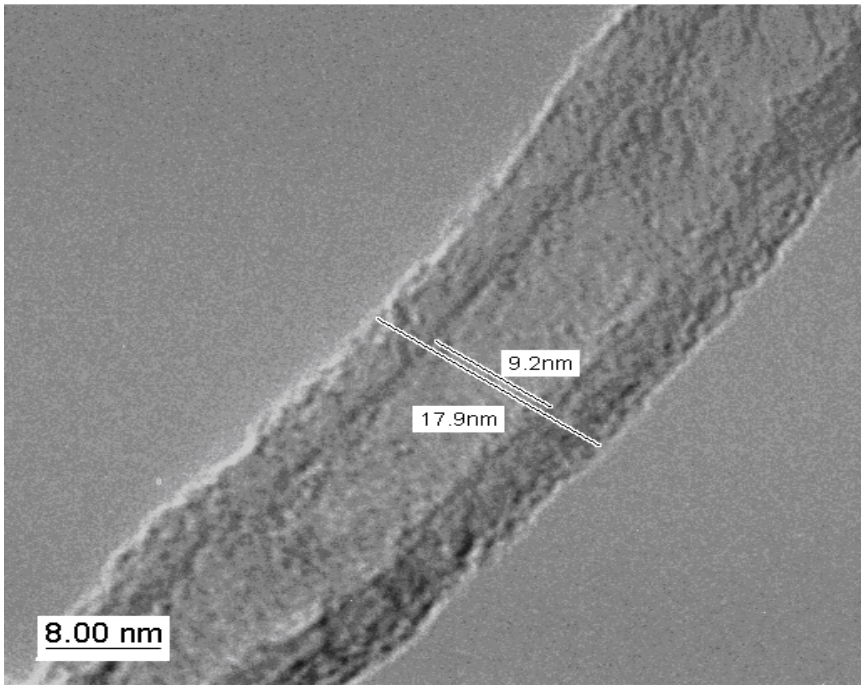

Figure 4.12: High magnification image of CNT sample showing diameter of the nanotube and the thickness of the multiwalls.

4.4 Purification of the Carbon Nanotubes

The CNT samples produced in the horizontal CVD reactor contain various impurities particularly the unreacted metal catalyst just like the ones synthesized in the SFCCVD reactor. These impurities, which are mainly residual metal catalysts, support materials and non–CNT microstructures e. g. amorphous carbon and fullerenes, impede the utilization of the unique properties of CNTs by poisoning the active components of the catalysts (Yu *et al.*, 1998; Lordi *et al.*, 2001). They have to be removed before the CNTs can be suitable as a support for platinum for use in catalyst electrodes in a fuel cell. Also, the as–synthesized CNTs usually have both ends closed which may hinder their adsorption and capillarity properties. Therefore, purification procedures should open both the tubes and eliminate the impurities. Among the various treatments that have been tested, a 1:3 solution of nitric and sulphuric acid has proven to be the most effective for modification of the CNT surface with the formation of functional groups (Porro *et al*., 2007).

Figure 4.13 shows the comparative TEM images of the as-synthesized and purified CNT samples. From the surface morphology of the images shown in this figure, it can be seen that the as-prepared CNT samples contained impurities such as amorphous carbon, and iron and cobalt particles. Amorphous carbon impurities are known to form from low temperature decomposition of carbon source during CVD production of CNTs, while metal impurities resulted from the metal catalyst particles that were unreacted during the synthesis of these materials.

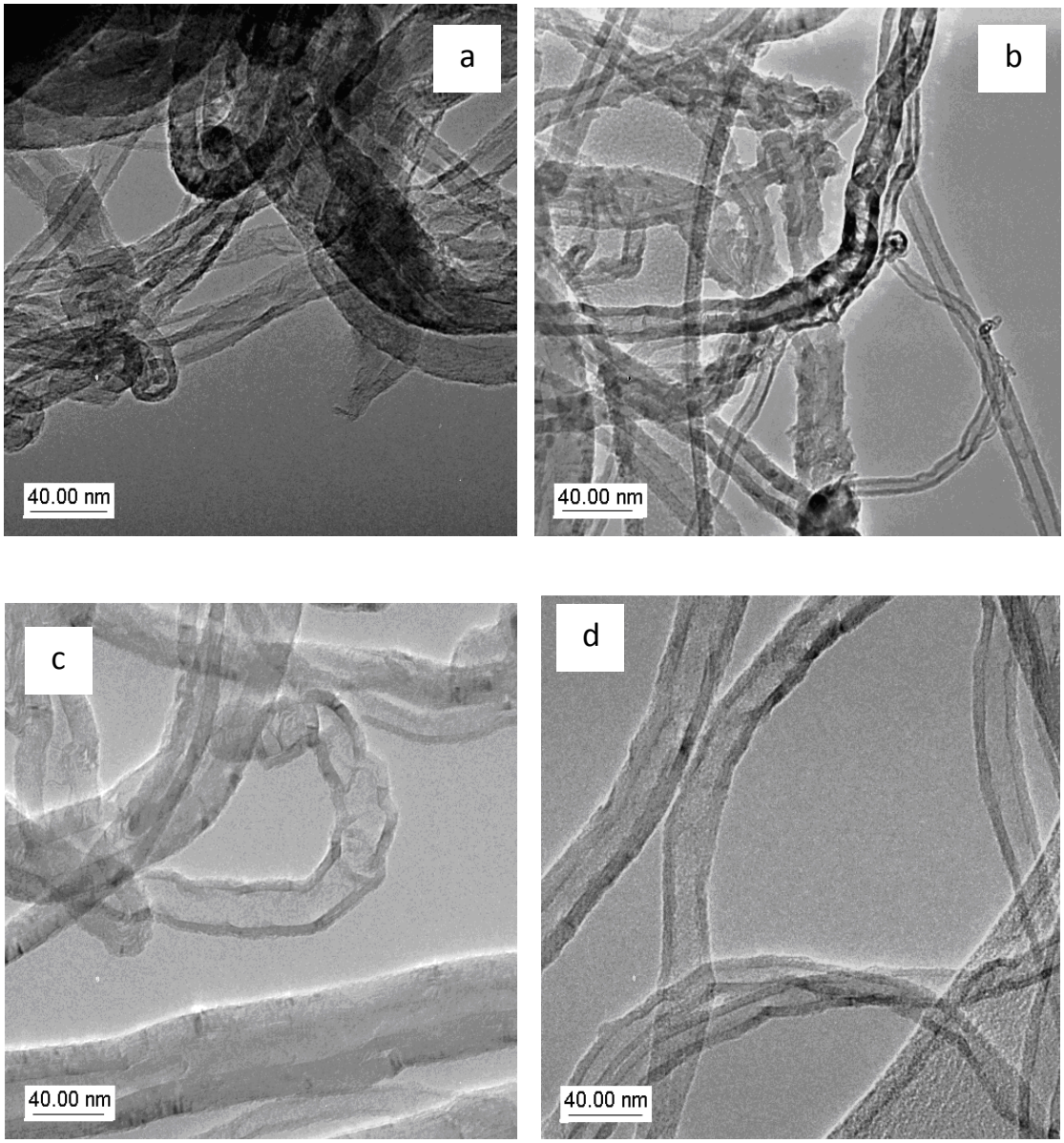

Figure 4.13: TEM images of (a–b) as–synthesized and (c–d) purified CNT samples.

The tiny black particles shown within the matrix of these materials as revealed in the figure are iron and cobalt particles as confirmed by EDX analysis shown in Figure 4.11. These metallic impurities were the residues from the metal catalyst used to synthesize the

CNTs. It was suspected that the residue from the support ($CaCO_3$) used to prepare the Fe–Co catalyst might also be a source of impurity. Hence a mixture of concentrated nitric and sulphuric acids was used to effect the purification and induce the formation of functional groups on the CNT samples (Rosca *et al.,* 2005; Porro *et al.,* 2007). During the high temperature synthesis of the CNTs, the calcium carbonate support for the iron and cobalt catalyst decomposed into calcium oxide (CaO) and carbon dioxide as shown in equation 4.2

$$CaCO_3(s) = CaO(s) + CO_2(g) \quad (4.2)$$

Thus traces of calcium oxide are likely to be present within the synthesized CNT samples. During the acid treatment, this metal oxide was neutralized by the high concentration of nitric acid used and produce soluble calcium nitrate and sulphate (Equation 4.3) which was easily removed as;

$$CaO(s) + 2HNO_3(aq) = Ca(NO_3)_2(aq) + H_2O(l) \quad (4.3)$$

$$CaO(s) + H_2SO_4(aq) = CaSO_4(s) + H_2O(l) \quad (4.4)$$

It has been found that about 4 ml of nitric acid is required to dissolve 1 g of CaO (Motchelaho, 2008), but for effective purification multiple quantities of a HNO_3/H_2SO_4 acid mixture were employed. Since the quantity of the nitric acid was triple that of the sulphuric acid, it is therefore believed that equation (4.3) is more likely to occur. This reaction favours the purification process since $CaSO_4$ is sparingly soluble while $Ca(NO_3)_2$ is readily soluble in water. The soluble impurities were filtered off during the

purification process to obtain pure CNT samples. Iron and cobalt impurities were also dissolved in the manner similar to the equations above and their respective soluble products were filtered off. Any traces of amorphous carbon were readily oxidized at high temperature during the thermal treatment of the CNTs (Ajayan *et al.*, 1993; Yao *et al.*, 1998). EDX analysis of the purified CNT samples shown in Figure 4.14 also confirmed total removal of these metallic impurities from the samples.

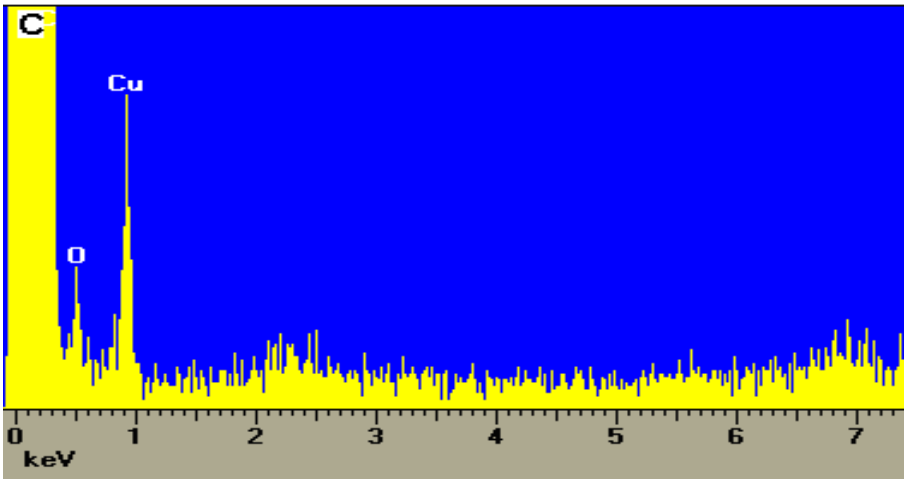

Figure 4.14: EDX analysis of the purified CNT sample.

The purification process also oxidizes the CNTs to produce functional groups (Ajayan *et al.*, 1993; Yao *et al.*, 1998; Rosca *et al.*, 2005). The high acid concentration of the acids used has an influence on the CNT solubility. Mawhinney *et al.* (2000), Hu *et al.* (2001) and Rosca *et al.* (2005) have shown that the affinity of the HNO_3 acid towards the amorphous and crystalline carbon depends strongly on its concentration; hence the high concentration of the acids employed in this work produced effective purification and oxidation of the CNT samples.

4.5 Raman Spectroscopy Studies of Carbon Nanotubes Produced

Raman spectroscopy (RS) is an effective way to evaluate the quality of CNTs. The Raman spectra of the purified and unpurified CNT samples shown in Figure 4.15 indicate two main peaks at around 1350 and 1600 cm $^{-1}$ which are designated as the D–band and G–band (Yoshikawa *et al*., 1998; Yoshikawa *et al*., 2004). The D– band represents the disorder – induced mode while the G – band can be attributed to a C–C stretching mode of well graphitized CNTs (Kastner *et al.*, 1994; Rao *et al.*, 1997; Kibria *et al.*, 2002).

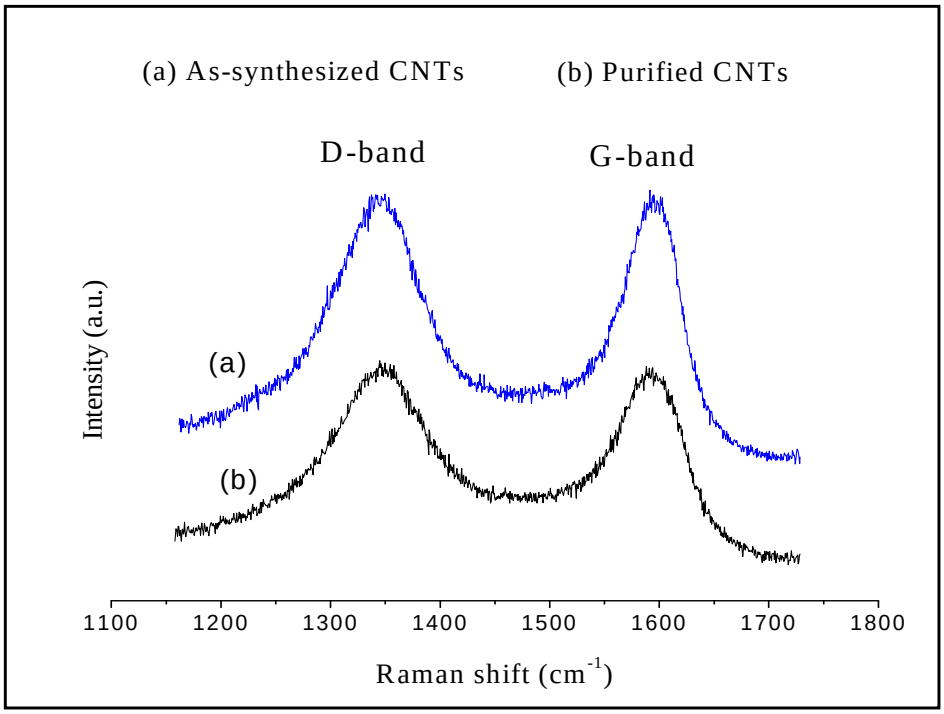

Figure 4.15: Raman spectra of purified and unpurified CNT samples.

The purified CNT sample shows broader peaks for both D and the G modes than the as–synthesized sample. This indicates that the purified CNT sample contains low level of

impurities. The relative intensity ratio of the D and G bands $\left(\frac{I_D}{I_G}\right)$, is known to depend on the structural characteristics of carbon (Kastner *et al.,* 1994). As the $\left(\frac{I_D}{I_G}\right)$ ratio increases, the defect structure increases and the degree of graphitization becomes less. The $\left(\frac{I_D}{I_G}\right)$ ratios of 0.86 and 0.85 were obtained for unpurified and purified CNT samples respectively which show that the purification process improves the crystallization of the CNTs. This ratio gives information about the perfection of the graphite layer structure and reflects the properties of the edge plane or boundary of the graphite crystal faces. As the $\left(\frac{I_D}{I_G}\right)$ ratio increases, the defect structure increases and the degree of graphitization becomes less (Wang *et al.,* 2004).

4.6 Thermogravimetry Analysis of Carbon Nanotubes Produced

Thermogravimetric analysis (TGA) can be used to examine the kinetics of a chemical process as well as the percentage weight and derivative weight change in the sample as a function of temperature (Okpalugo *et al.,* 2005). Figure 4.16 shows the TGA curves of the purified and as – synthesized CNT samples which were carried out in an oxygen atmosphere to monitor the weight loss and thermal stability of the samples. These analyses were carried out by heating about 15 mg of CNT sample under a continuous flow of air. The temperature was initially held at 25°C for 1 min before being heated to 900°C at the rate of 10°C/min.

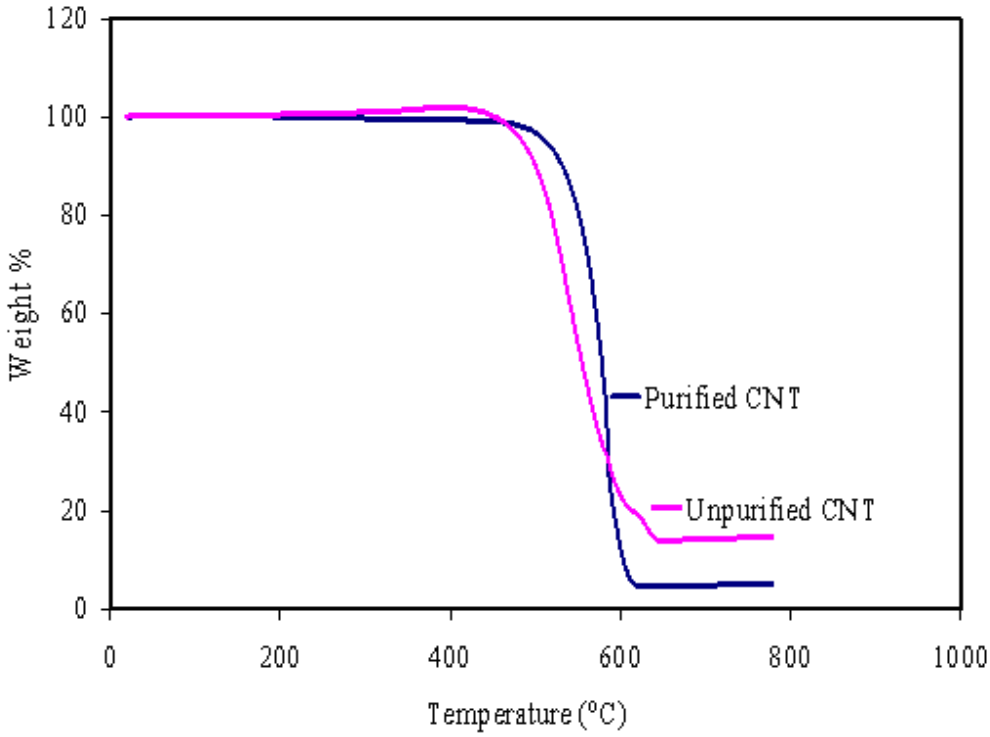

Figure 4.16: TGA curves of purified and unpurified CNT samples.

The TGA curve for the purified CNT sample shows a mass loss of 98% at T < 500°C which indicates that is relatively pure. Since amorphous carbons were expected to have been oxidized during acid and thermal treatment, the 2% impurity is suspected to be due to residue metallic partic3les, which were possibly trapped within the tubes and could not be removed by acid treatment. On the other hand, the curve for the as–synthesized CNT sample shows a mass loss of 83% (starting at a much lower temperature of 450°C). This behaviour can be traced to the presence of impurities, particularly the presence of traces of support in this sample.